

Boron-dipyrromethene based multi-anionic sensor and a specific cationic sensor for Fe³⁺†

Vellanki Lakshmi and Mangalampalli Ravikanth*

Cite this: *J. Mater. Chem. C*, 2014, 2, 5576Received 17th February 2014
Accepted 14th March 2014

DOI: 10.1039/c4tc00317a

www.rsc.org/MaterialsC

Symmetrical and unsymmetrical phenylhydrazone substituted boron-dipyrromethenes were synthesized by treating 3,5-diformyl boron-dipyrromethene with phenylhydrazine/2,4-dinitrophenylhydrazine in ethanol at reflux temperature. The X-ray structure of the unsymmetrical boron-dipyrromethene (BODIPY) was shown to have an almost extended planar orientation of BODIPY with 2,4-dinitrophenylhydrazone unit at the 3-position and ethyl acetal at the 5-position with small torsional angles. A strong absorption band at ~600 to 700 nm and a weak emission band at ~620 to 710 nm were observed for the phenylhydrazone substituted BODIPYs. The compounds showed interesting absorption properties in DMSO and DMF solvents compared to other solvents by shifting ~150 nm towards the red region. Anion binding studies indicated that the unsymmetrical phenylhydrazone substituted BODIPY could be applied as a sensor for F⁻, CH₃COO⁻ and H₂PO₄⁻ ions as confirmed by various spectroscopic studies. Furthermore, the unsymmetrical phenylhydrazone substituted BODIPY had the unique ability of acting as a two step fluorescence enhanced chemodosimetric sensor for Fe³⁺ ion.

Introduction

There are numerous applications of boron-dipyrromethene (BODIPY) dyes in fields ranging from materials to medicine because of their excellent thermal, chemical and photochemical stability, high molar absorptivity, high fluorescence quantum yields and low sensitivity to both solvent polarity and pH.¹ The properties of BODIPY dyes can be fine tuned by introducing appropriate substituents at the BODIPY core. Thus, BODIPY dyes are amenable for functionalization, and the functionalized BODIPYs have been used to synthesize a wide variety of substituted BODIPYs for various applications.² For example, halogenated BODIPYs have been used as synthons for the synthesis of a variety of polyarylated BODIPYs^{3a-c} and cascade type BODIPY arrays.^{3d,e} Ziesel *et al.* developed a route to introduce ethynyl functional groups in place of fluorides in BODIPY and used these systems to produce very interesting light-harvesting systems.⁴ We recently reported the synthesis of 3,5-diformyl BODIPYs under simple reaction conditions and used them to prepare a pH-based optical sensor⁵ as well as for sensing CN⁻ ion by using various spectroscopic methods.⁶ We also reported the synthesis of 3,5-bis(dipyrromethanyl) BODIPYs by treating 3,5-diformyl BODIPYs with excess pyrrole in the presence of mild acid and demonstrated their use as an

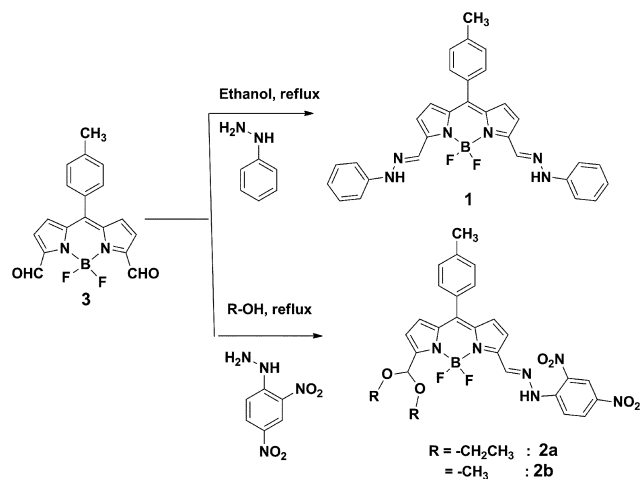
exclusive sensor for F⁻ ion.⁷ However, the aldehyde functional group on the BODIPY core enables the synthesis of novel substituted BODIPYs which will be useful for a range of applications.⁸ Here we report the synthesis of phenylhydrazone and 2,4-dinitrophenylhydrazone substituted BODIPYs **1** and **2** respectively by treating 3,5-diformyl BODIPY **3** with appropriate phenylhydrazines in alcohol at refluxing temperature. Our studies indicated that compound **1** cannot sense anions whereas compound **2** can bind to anions such as F⁻, CH₃COO⁻, and H₂PO₄⁻ as confirmed by optical and NMR techniques. Furthermore, we also showed that BODIPY **2** acts as a two step fluorescence enhanced sensor which is unique and different from other fluorescence enhanced Fe³⁺ sensors reported in the literature.⁹

Results and discussion

The phenylhydrazone substituted BODIPYs **1**, **2a** and **2b** were synthesized as outlined in Scheme 1. Compound **1** was synthesized by treating 3,5-diformyl BODIPY⁵ **3** with two equivalents of phenylhydrazine in ethanol at refluxing temperature for 5 h. TLC analysis of the reaction mixture indicated the disappearance of spots corresponding to the precursors and the appearance of one desired major violet spot along with two unidentified minor spots. The crude compound was subjected to alumina column chromatography and afforded the desired compound **1** in 62% yield as a blue solid. Compound **2a** was prepared similarly by treating **3** with two equivalents of 2,4-dinitrophenylhydrazine in ethanol at reflux for 5 h whereas compound **2b** was prepared by changing the solvent from

Department of Chemistry, Indian Institute of Technology Bombay, Powai, Mumbai 400 076, India. E-mail: ravikanth@chem.iitb.ac.in

† Electronic supplementary information (ESI) available: Experimental methods, spectral data, fluorescence, absorption spectral traces. CCDC 945253. For ESI and crystallographic data in CIF or other electronic format see DOI: 10.1039/c4tc00317a



Scheme 1 Synthesis of compounds 1, 2a and 2b.

ethanol to methanol. The crude compounds were subjected to alumina column chromatography and afforded pure **2a** and **2b** in 17 and 26% yields respectively. Interestingly, when we used 2,4-dinitrophenylhydrazine, we obtained only monohydrazone substituted BODIPY and the aldehyde at the 5-position was converted to acetal. We did not notice the formation of any dihydrazone substituted compound in this reaction even when we used excess equivalents of 2,4-dinitrophenylhydrazine. Compounds **1**, **2a** and **2b** were freely soluble in common organic solvents and the molecular structures were confirmed by HR-MS, NMR and the crystal structure determined for compound **2a**.

Compounds **1**, **2a** and **2b** were characterized in detail by ^1H , ^{19}F , ^{11}B and $^1\text{H}-^1\text{H}$ COSY NMR spectroscopy. The ^1H NMR of compounds **1**, **2a** and **2b** were recorded in a hydrogen bond donating solvent (HBD) such as CDCl_3 and a hydrogen bond accepting solvent (HBA) such as $\text{DMSO}-d_6$ and a comparison of compounds **1** and **2a** in two different solvents is presented in Fig. 1a. Furthermore, the $^1\text{H}-^1\text{H}$ COSY NMR spectrum of compound **2a** is presented in Fig. 1b. In the ^1H NMR spectrum of compound **1** in CDCl_3 , four pyrrole signals due to the BODIPY core (f, g, h, i type) appeared as two sets of signals at 6.81 and 7.11 ppm because of symmetric substitution; the alkene CH proton appeared as a singlet at 8.20 ppm and the NH proton appeared as a singlet at 8.49 ppm. In the ^1H NMR spectrum of compound **2a**, the four pyrrole protons (f, g, h, i type) appeared as four different sets due to unsymmetric substitution. These protons were identified with the help of cross peak correlations observed in the $^1\text{H}-^1\text{H}$ COSY NMR spectrum (Fig. 1b). The alkene CH proton and acetal CH proton of compound **2a** were observed at 8.61 and 5.98 ppm respectively. All the aryl signals were also identified based on cross-peak correlations observed in the $^1\text{H}-^1\text{H}$ COSY NMR spectrum. Similar NMR features to those observed for compound **2a** were observed for compound **2b**. The most interesting feature in the spectrum of compound **2** is the NH proton which appeared as a singlet at 11.6 ppm. The NH proton in compound **2** was down field shifted by 3.2 ppm compared to that of compound **1** supporting the strong

intramolecular hydrogen bonding between NH and NO_2 groups in compound **2**. The ^1H NMR spectra of compounds **1** and **2a** recorded in $\text{DMSO}-d_6$ had the same number of signals with slight shifts in their chemical shifts except for the NH proton which experienced a downfield shift compared to that recorded in CDCl_3 . For example, the NH proton of compound **1** which appeared at 8.49 ppm in CDCl_3 experienced a 3 ppm downfield shift and appeared at 11.5 ppm in $\text{DMSO}-d_6$. Similarly, the NH proton of compound **2a** and **2b** was also downfield shifted by ~ 1 ppm in $\text{DMSO}-d_6$ compared to that recorded in CDCl_3 . Furthermore, the magnitude of the downfield shift of the NH proton of compound **1** was much larger compared to that of compounds **2a** and **2b** when the solvent was changed from CDCl_3 to $\text{DMSO}-d_6$ (Fig. 1a). This is attributed to the strong intermolecular hydrogen bonding present between the hydrazone NH of compound **1** and the oxygen atom of the solvent. However, in compounds **2a** and **2b**, since the hydrazone NH is already engaged in intramolecular hydrogen bonding with the NO_2 group, an additional 1 ppm downfield shift was observed due to intermolecular hydrogen bonding interaction with the solvent. Furthermore, compounds **1**, **2a** and **2b** were also characterized by ^{19}F and ^{11}B NMR techniques. In the ^{19}F NMR spectra, a broad signal at -138 ppm was observed for compound **1** but a typical quartet at ~ -138 ppm was observed for compounds **2a** and **2b**. In the ^{11}B NMR spectra, a triplet at ~ 1.0 ppm was observed for compounds **1**, **2a** and **2b** which was slightly downfield shifted compared to that observed for other BODIPYs such as *meso*-phenyl BODIPY 10 (0.5 ppm).

The structure of compound **2a** was unambiguously characterized by X-ray diffraction analysis. Single crystals of **2a** suitable for X-ray analysis were grown by vapour diffusion of petroleum ether into CHCl_3 solution under atmospheric pressure over a period of 15 days. Compound **2a** was crystallized \ddagger with monoclinic symmetry and a $C2/c$ space group. The crystal structure is depicted in Fig. 2. The structure is shown to have an almost extended planar orientation of BODIPY with a phenylhydrazone unit on one side and ethyl acetal on the other side, and small torsional angles of 8.1° ($\text{C}_{15}, \text{C}_{16}, \text{C}_{17}, \text{N}_3$) and 4.1° ($\text{N}_3, \text{N}_4, \text{C}_{18}, \text{C}_{19}$) respectively. The dipyrin core of compound **2a** exhibits a planar conformation having a central six-membered ring fused with two adjacent five-membered rings. The two fluoride atoms present on the boron atom of the central six-membered ring as well as the alkoxy substituents of the acetal functional group are perpendicular to the dipyrin core. The dihedral angle between the *meso*-substituted phenyl group and dipyrin unit is 69° and the B-N bond distances are approximately 1.54 Å which indicates the usual delocalization of the positive charge on both the nitrogen atoms as noted for other BODIPYs. 10 Furthermore, compound **2a** displays some secondary intramolecular interactions such as $\text{C}-\text{H}\cdots\text{F}$ (2.65 Å) between B-F and the $\text{H}-\text{C}_{17}$ carbon, and $\text{N}_4-\text{H}\cdots\text{O}_3$ (1.96 Å) between N_4-H and *ortho*-substituted NO_2 group in dinitrophenylhydrazone unit which probably plays a crucial role in the planarization of the molecule (Fig. 2). In addition, multiple $\text{C}-\text{H}\cdots\text{F}$ and $\text{N}-\text{H}\cdots\text{F}$ intermolecular interactions were also observed due to the strong electronegativity of F and N atoms which led to a supramolecular head to tail assembly (Fig. 3). For

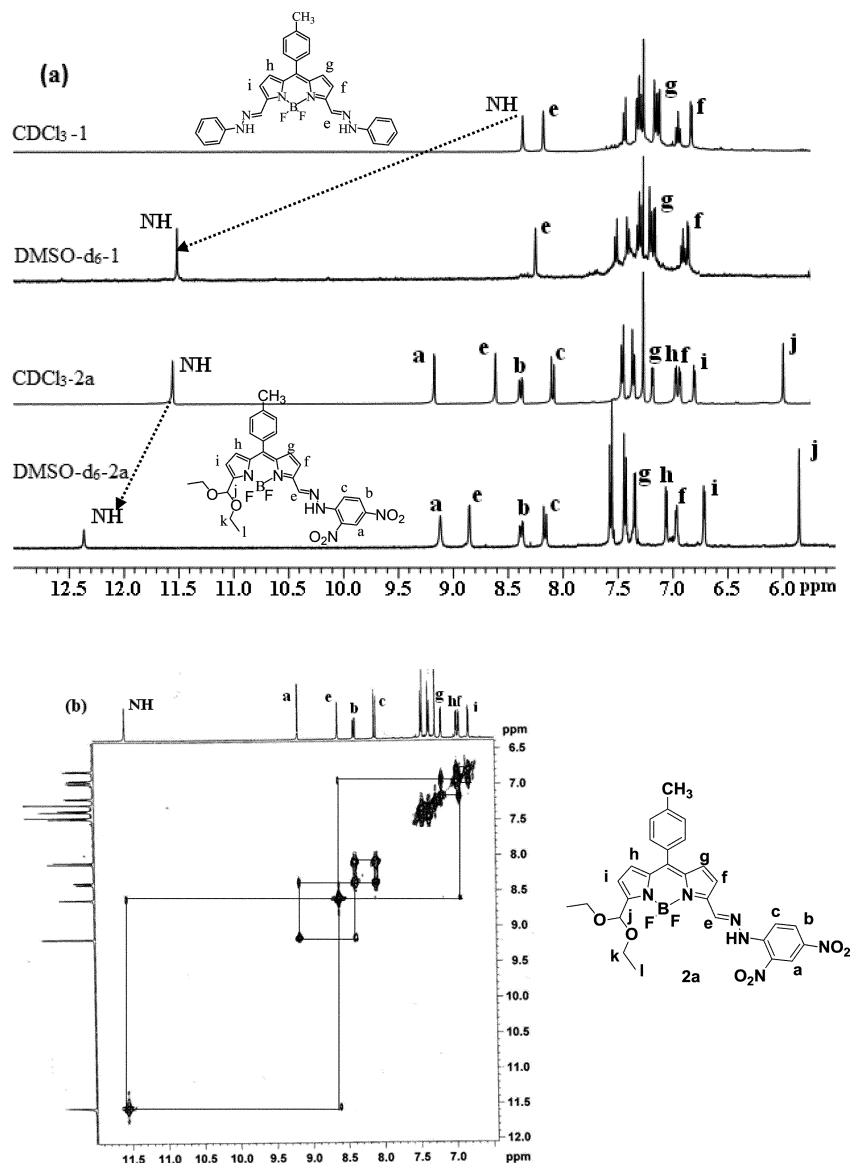


Fig. 1 (a) Comparison of ¹H NMR spectra of compounds 1 and 2a in CDCl₃ and DMSO-d₆. (b) ¹H-¹H correlation spectrum of compound 2a in CDCl₃.

instance, out of the two fluorides which were arranged above and the below the plane of BODIPY, one fluoride was involved in intermolecular hydrogen bonding with the NH atom of one adjacent molecule while the other fluoride was involved in intermolecular hydrogen bonding with the hydrogen atom of the *meso*-tolyl CH₃ group of another BODIPY molecule with bond distances in the range of 2.51 Å to 2.64 Å (Fig. 3).

The absorption properties of compounds 1 and 2a were studied in different solvents of varying polarity. A comparison of the absorption spectra of compounds 1 and 2a recorded in CHCl₃ and DMSO is presented in Fig. 4 and the relevant absorption data measured in different solvents are presented in Table 1. A typical strong S₀ → S₁ transition in the 600–650 nm region with a vibronic component at higher energy along with a broad S₀ → S₂ transition at ~400 nm were observed for compounds 1 and 2 as were observed for *meso*-phenyl BODIPY.¹⁰ Compound 1 absorbs

at a higher wavelength due to the presence of two phenylhydrazone units leading to more π-delocalization compared to the one phenylhydrazone unit present in compound 2. The solvent study showed that compounds 1 and 2 exhibited a regular hypsochromic shift with an increase of the polarity of the solvent as noted for BODIPY systems.¹⁰ However, we noted a large bathochromic shift in the absorption band of compounds 1 and 2 in hydrogen bonding accepting solvents such as DMSO and DMF. The absorption band at 682 nm in CHCl₃ observed for compound 1 was bathochromically shifted by 50 nm in DMSO and appeared at 712 nm (Fig. 5a). Interestingly, the absorption band observed for compound 2 experienced a large red shift of 172 nm (Fig. 5b) when the solvent was changed from CHCl₃ to DMSO. The red shifts observed for compounds 1 and 2 in DMSO/DMF were attributed tentatively to the stabilization of the energy states due to hydrogen bonding interaction between the NH of

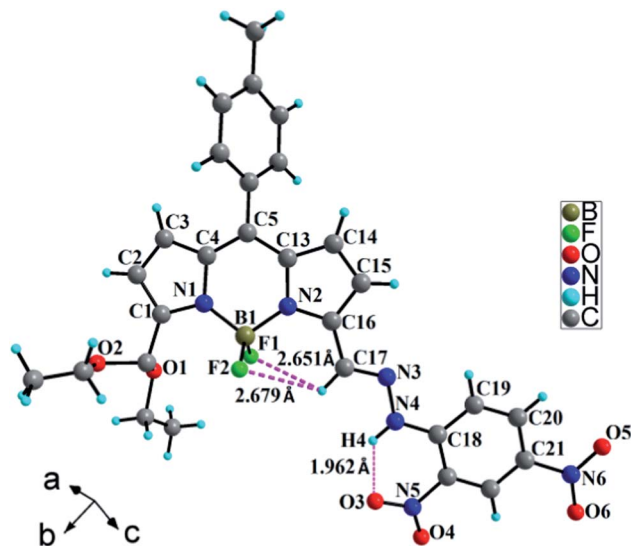


Fig. 2 Crystal structure of compound 2a with intramolecular hydrogen bonding interactions. The solvent molecules are omitted for clarity.

the compounds with the solvents resulting in the reduction of the HOMO–LUMO gap. The large red shift observed for compound 2 supports the stronger hydrogen bonding interaction between the solvent and compound 2.

Anion binding studies

It has been shown in the literature that dinitrophenylhydrazone substituted fluorophores bind to anions.¹¹ To test the ability of compounds 1 and 2 to sense anions such as F^- , Cl^- , Br^- , I^- , N_3^- , NO_3^- , HSO_4^- , ClO_4^- , HPO_4^{2-} , $H_2PO_4^-$, HCO_3^- , CH_3COO^- , we first qualitatively carried out studies by adding excess equivalents of various anions to 1 and 2 in CH_3CN and followed the changes by absorption spectroscopy (Fig. 6). The addition of F^- , CH_3COO^- and $H_2PO_4^-$ ions to compound 2a resulted in a colour change from violet to light transparent green with a significant bathochromic shift (~ 160 nm) in the absorption maxima whereas all the other anions listed above did not show

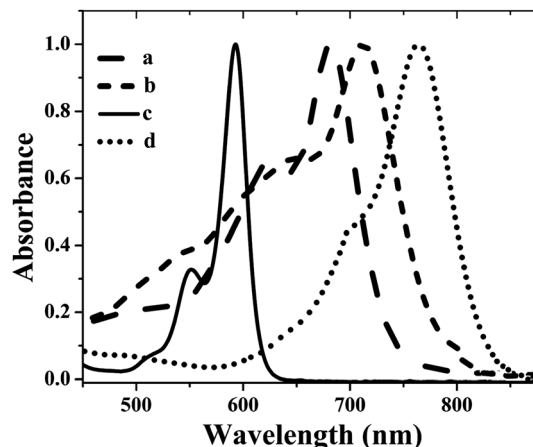


Fig. 4 Comparison of the absorption spectra of compound 1 in (a) $CHCl_3$ (dashed line) and (b) DMSO (small dashed line), and compound 2a in (c) $CHCl_3$ (solid line) and (d) DMSO (dotted line).

Table 1 Photophysical data for compounds 1 and 2a

Solvent ^a	Compound 1		Compound 2a	
	λ_{max} (log ϵ_{max})	FWHM	λ_{max} (log ϵ_{max})	FWHM
Toluene	691 (4.55)	593 (6.06)	910	2773
$CHCl_3$	682 (4.56)	592 (6.06)	950	2774
MeOH	684 (4.54)	587 (6.04)	1033	3070
CH_3CN	690 (4.57)	586 (6.00)	971	2884
DMF	703 (4.50)	762 (6.05)	1407	3691
DMSO	712 (4.47)	764 (6.05)	1506	3676

^a Dielectric constant: toluene = 2.4, chloroform ($CHCl_3$) = 4.8, methanol = 32.7, acetonitrile (CH_3CN) = 37.5, dimethylformamide (DMF) = 36.7, dimethyl sulfoxide (DMSO) = 46.7.

any change in the absorption peak maxima indicating that compound 2a acts as an optical sensor for three anions, namely, F^- , CH_3COO^- and $H_2PO_4^-$ ions (Fig. 6). The addition of these three anions to compound 1 in CH_3CN also changed the position of the absorption band but the magnitude of the shift was much less (50 nm) and the absorption band was very much

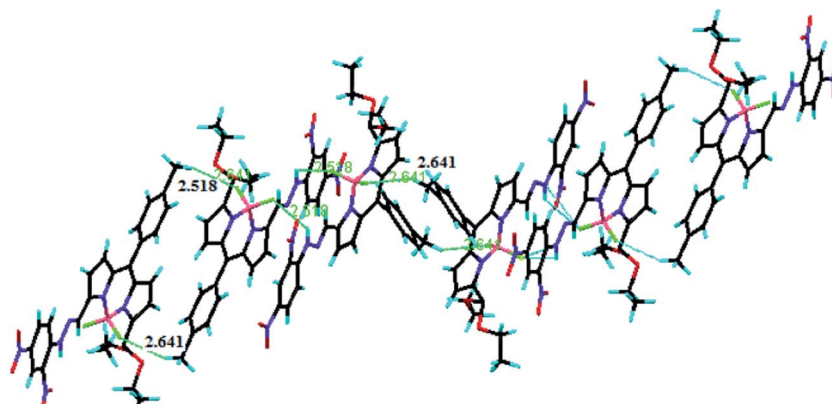


Fig. 3 Supramolecular assembly of compound 2a through intermolecular-hydrogen bonding network (between $H10b \cdots F2$ and $F1 \cdots H4$).

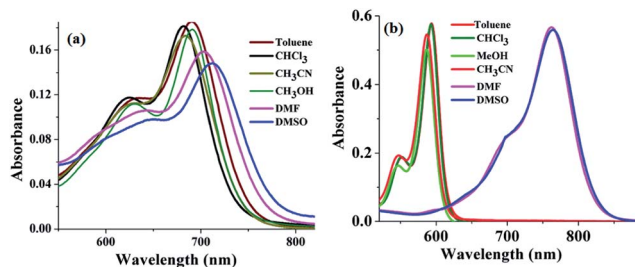


Fig. 5 Absorption spectra of (a) compound 1 and (b) compound 2a in various solvents.

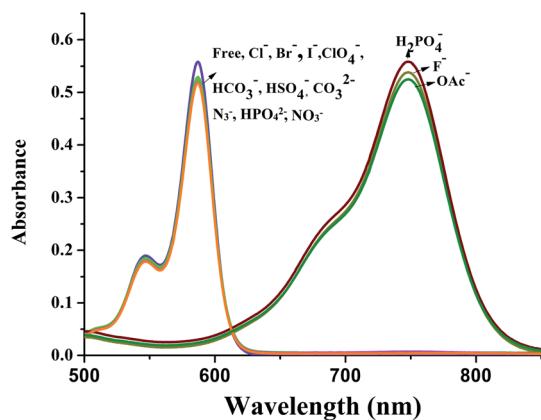


Fig. 6 Absorption spectra of compound 2a (5×10^{-6} M) in the presence of various anions (50 equivalents) in CH_3CN .

broadened. Hence, systematic anion sensing experiments were not carried out further with compound 1. Thus, we carried out the absorption spectral titration of compound 2a with increasing amounts of F^- , CH_3COO^- and H_2PO_4^- ions and the systematic changes in the absorption spectrum of compound 2a on addition of increasing amounts of tetrabutylammonium fluoride (TBAF) in CH_3CN are shown in Fig. 7a. The addition of F^- to a CH_3CN solution of compound 2a resulted in a decrease of the absorption band at 586 nm and the appearance of a new band at 747 nm with a clear isosbestic point at 613 nm indicating that compound 2a acts as a F^- sensor in solution. This was also clearly evident in the plot which shows the changes in the absorption bands at 586 and 747 nm *versus* the amount of F^- ion (Fig. 7a inset). Similar absorption spectral changes with clear isosbestic points were also noted for the systematic addition of CH_3COO^- (Fig. S14[†]) and H_2PO_4^- (Fig. S15[†]) ions to compound 2a supporting the conclusion that compound 2a also acts as a sensor for these two anions.

The large bathochromic shifts of the absorption band maxima of compound 2a upon binding with F^- , CH_3COO^- and H_2PO_4^- ions was tentatively attributed to the removal of the NH proton of the dinitrophenylhydrozone group (Scheme S1[†]) by the anion. This resulted in an increase of the electron density on nitrogen and participates in delocalization with the dinitrophenyl group leading to a more stable delocalized structure. Thus, the electrons are rearranged in the whole molecule and

the π -electron delocalization extends all over the molecule leading to a significant bathochromic shift. A job plot analysis of sensor 2a with F^- interaction supports the 1 : 1 binding stoichiometry (Fig. 7c). The binding constant evaluated from the Benesi-Hildebrand equation was found to be 3×10^3 , 2.6×10^3 and 9×10^3 for F^- , H_2PO_4^- and CH_3COO^- ions respectively on interaction with compound 2a. We also followed the interaction of F^- ion with 2a by fluorescence spectroscopy as shown in Fig. 7b. It is clear from Fig. 7b that the intense fluorescence peak at 609 nm was completely quenched upon addition of 8 equiv. of F^- to compound 2a. However, we noted the significant change in the fluorescence spectrum of compound 2a upon addition of 2 equiv. of F^- ion. Furthermore, the addition of F^- , AcO^- and H_2PO_4^- ions to compound 2a changes the colour of the solution from violet to faded green, whereas no colour change was noted in the presence of other anions (Fig. 8a).

To further elucidate the nature of the interaction between the anions and compound 2a, we carried out a ^1H NMR titration of compound 2a in CD_3CN upon addition of TBAF ion, and the ^1H NMR spectral changes are displayed in Fig. 9. Upon the gradual addition of F^- ion, the NH signal at 11.5 ppm disappeared completely supporting the deprotonation mechanism. The removal of the proton from NH by the anion results in an increase of the electron density on nitrogen which is then propagated through delocalization into the 2,4-dinitrophenyl motif resulting in an increase of the electron density in the entire molecule. The increase in the electron density causes a shielding effect leading to upfield shifts of protons such as H_a – H_f which are closer to the anion binding site. The other protons of the BODIPY moiety which are far from the anion binding site showed negligible shifts. Thus, ^1H NMR titration studies confirmed that NH was involved in binding with the F^- ion and that anion binding causes deprotonation which increases the delocalization in the molecule and results in a large red shift of the absorption band and upfield shifts in the ^1H NMR.

The binding of 2a with F^- ion was also further probed by following the changes in the reduction of compound 2a upon addition of F^- ion using square wave voltammetry. Fig. 10 shows the systematic changes in the reduction waves of compound 2a upon the addition of increasing amounts of fluoride ion. As is clear from Fig. 10 the addition of increasing amounts of F^- ion to 2a resulted in a decrease of the intensity of the reduction waves at -0.48 V and -0.82 V with a gradual increase in the reduction wave appearing at -0.66 V. The complete disappearance of the reduction wave at -0.48 V with an increase in the intensity of the reduction wave at -0.66 V indicates that the interaction of F^- ion with 2a makes the boron-dipyrromethene unit of 2a relatively more electron rich due to deprotonation of the hydrozone unit. Similar observations were made for the anions AcO^- and H_2PO_4^- . However, no change in the reduction of 2a was observed upon addition of any other anions. Thus, the electrochemical study was in agreement with the absorption and fluorescence spectroscopic studies and supports the conclusion that 2a can also be used as an electrochemical sensor for F^- , AcO^- and H_2PO_4^- ions.

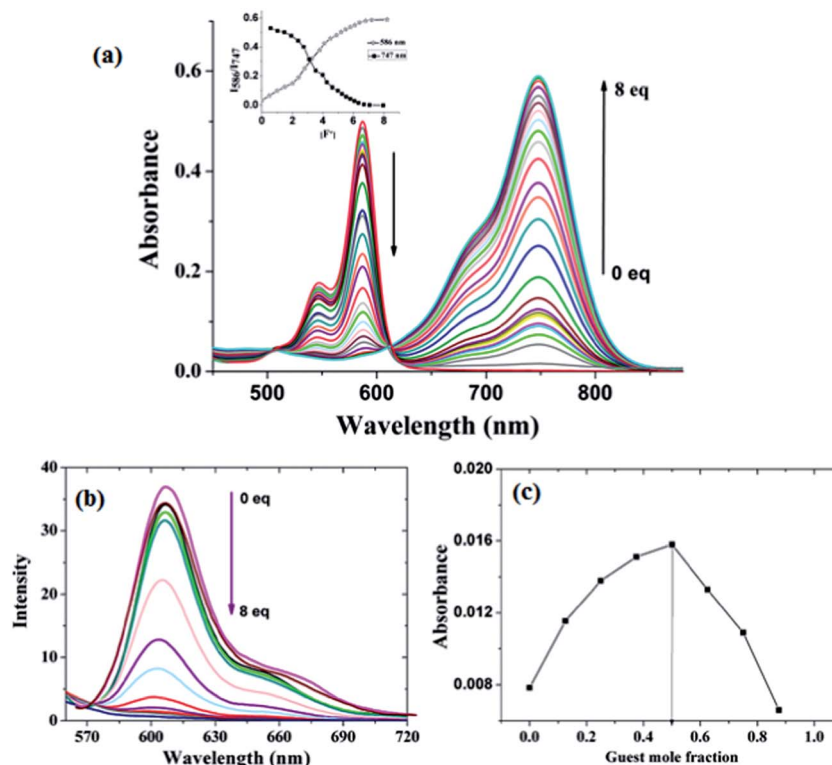


Fig. 7 (a) Absorption spectra of compound **2a** (5×10^{-6} M), with different concentrations of F^- (TBAF) solution (0–8 equiv.) in CH_3CN . Inset is a plot of A_{586}/A_{747} vs. $[F^-]$. (b) Emission spectral changes of BODIPY **2a** ($5 \mu M$) upon addition of increasing equivalents of F^- ion ($\lambda_{ex} = 530$ nm). (c) Job plots of **2a** (at 586 nm) with F^- anion. The total concentration of the host and guest is 1.0×10^{-4} mol L^{-1} in CH_3CN .

Cation sensing studies

To obtain an insight into the sensing properties of compound **2a** towards various metal ions, we studied the effects of the addition of different metal ions such as Li^+ , Na^+ , K^+ , Ca^{2+} , Mg^{2+} , Mn^{2+} , Cr^{3+} , Pb^{2+} , Co^{3+} , Pd^{2+} , Cu^{2+} , Hg^{2+} , Cd^{2+} , Ni^{2+} , Zn^{2+} , Fe^{2+} , Fe^{3+} to compound **2a** in CH_3CN solution and followed the changes by absorption and fluorescence spectroscopy. As shown in Fig. 11a, the absorption band of compound **2a** was hypsochromically shifted by 62 nm upon the addition of excess

equivalents (100 equivalents) of Fe^{3+} ion whereas no considerable changes in the position of the absorption band were observed upon the addition of any other metal ions. Similarly, the changes in the fluorescence spectra of compound **2a** upon the addition of different metal ions are shown in Fig. 11b. Compound **2a** exhibited negligible changes in the fluorescence intensities upon the addition of metal ions such as Li^+ , Na^+ , K^+ , Ca^{2+} , Mg^{2+} , Mn^{2+} , Cr^{3+} , Pb^{2+} , Co^{3+} , Pd^{2+} , Cu^{2+} , Hg^{2+} , Cd^{2+} , Ni^{2+} , Zn^{2+} but the addition of Fe^{2+} resulted in a considerable intensity

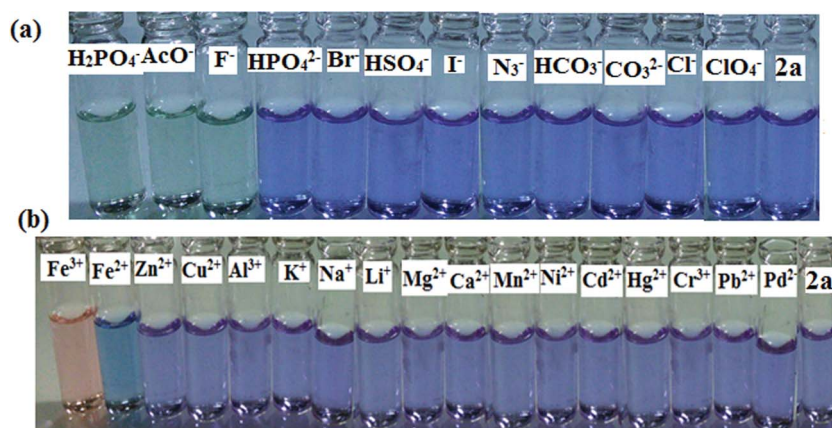


Fig. 8 Color change upon addition of excess equivalents of (a) various anions (tetrabutylammonium salts) and (b) various cations to BODIPY **2a** (1×10^{-5} M) in CH_3CN solution in daylight.

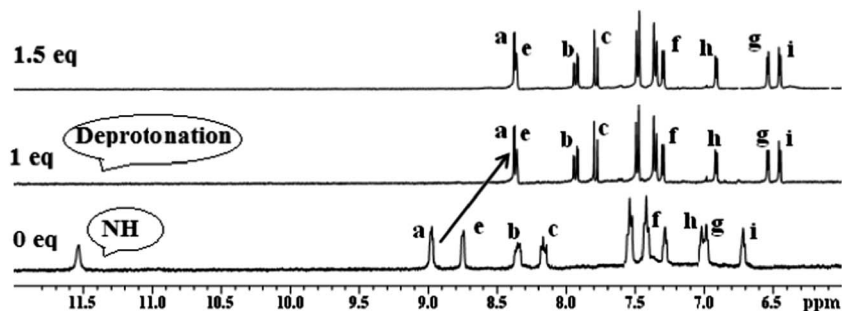


Fig. 9 Partial ^1H NMR spectrum of compound **2a** (2×10^{-2} M) in the presence of 1.5 equivalents of F^- ion in CD_3CN .

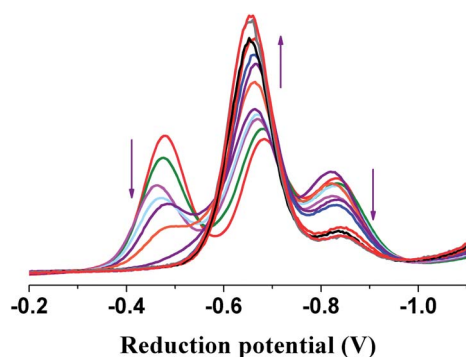


Fig. 10 Square wave voltammograms recorded at a scan rate of 50 mV s^{-1} of BODIPY **2a** (2 mM) in the presence of increasing amounts of F^- (TBAF) ions (0–1.2 equiv.) in CH_3CN containing 0.1 M TBAP as the supporting electrolyte.

change in the fluorescence spectra. However, a maximum fluorescence intensity enhancement with a 60 nm hypsochromic shift was observed for Fe^{3+} (Fig. 11b). Thus, the metal sensing studies indicated that compound **2a** was highly selective for Fe^{3+} which is attributed to the lower $\text{p}K_{\text{a}}$ of Fe^{3+} compared to other metal ions.¹¹ Our studies also indicated that compound **2a** can be used as a two step fluorescence enhanced

chemodosimetric sensor for Fe^{3+} which is different from the other reported⁹ chemodosimetric sensors for metals ions. This unique property of compound **2a** is due to the presence of two different substituents at the 3- and 5-positions, namely acetal and dinitrophenylhydrozone groups. The two different substituents on BODIPY **2a** were cleaved in a step-wise manner in the presence of Fe^{3+} and the changes that occurred due to the cleavage of the substituents are clearly observed (Fig. 8b) from the intensity enhancement of the fluorescence spectra. Thus, we demonstrated that the weakly fluorescent compound **2a** was converted to the highly fluorescent compound **3** via compound **4** in the presence of Fe^{3+} ion as described below.

The recognition of Fe^{3+} by compound **2a** was first scrutinized by UV-vis spectroscopy in CH_3CN . In the first step, upon addition of 0 to 1 equivalent of Fe^{3+} to compound **2a**, the absorption band at 586 nm was shifted bathochromically to 599 nm with a color change from violet to dark blue. An isosbestic point at 595 nm (Fig. 12a) was clearly observed upon increasing the concentration of Fe^{3+} up to 1 equivalent thus supporting the presence of two species in equilibrium. We reasoned that the two species which were in equilibrium were compound **2a** and its acetal hydrolyzed product, compound **4**. In the presence of the strong Lewis acidic Fe^{3+} ($\text{p}K_{\text{a}} = 2.83$),¹² the hydrolysis of the acetal group of compound **2a** to aldehyde was facilitated by

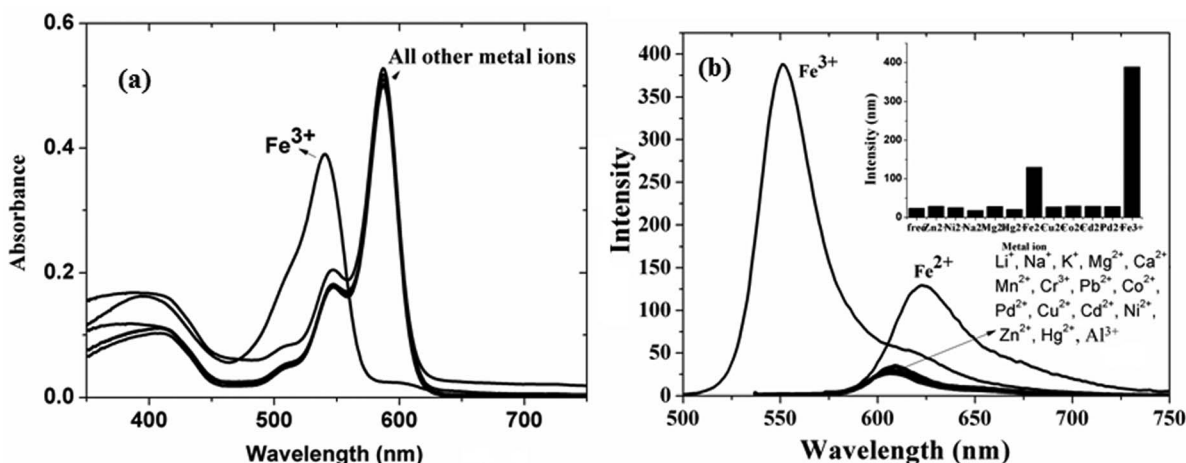


Fig. 11 (a) Absorption spectra and (b) emission spectra of compound **2a** excited at 488 nm in the presence of excess equivalents of various metal ions.

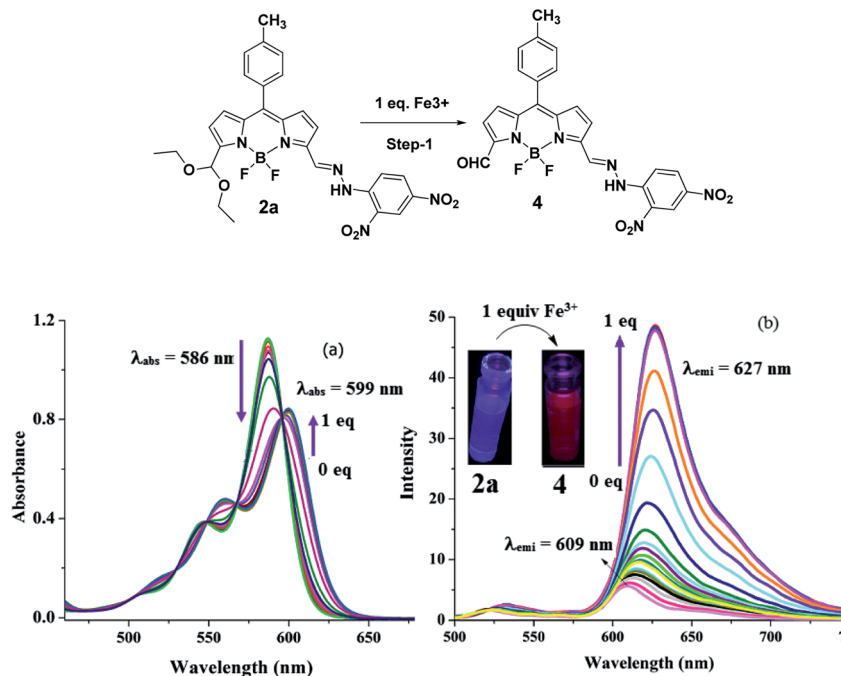


Fig. 12 (a) Absorption and (b) emission spectral changes of BODIPY 2a (10 μ M) upon titration with 0–1 equivalent of Fe³⁺ ($\lambda_{\text{ex}} = 488$ nm) in CH₃CN. (Inset: fluorescence colour change of 2a under a UV lamp ($\lambda_{\text{ex}} = 365$ nm) upon addition of 1 equivalent of Fe³⁺.)

coordinated acidic water molecules to form compound 4. We carried out the HR-MS analysis of compound 2a in the presence of one equivalent of Fe³⁺ and observed a molecular ion peak at 541.1242 (M + Na)⁺ thus confirming the formation of compound 4. The sensitivity of compound 2a towards Fe³⁺ was further investigated by fluorescence studies in CH₃CN. The fluorescence titration studies carried out by the addition of 0 to 1 equivalent of Fe³⁺ to compound 2a in CH₃CN are shown in Fig. 12b. In the absence of Fe³⁺, compound 2a was very weakly fluorescent ($\Phi_f = 0.006$) with a fluorescence maxima at 609 nm. Upon the addition of increasing amounts of Fe³⁺ to compound 2a, the weak fluorescence band of compound 2a at 609 nm was shifted bathochromically to 627 nm with a 10-fold intensity enhancement ($\Phi_f = 0.041$) which indicates the hydrolysis of the acetal group in compound 2a and the formation of compound 4. The weakly red fluorescent compound 2a was changed to a relatively more fluorescent compound upon the addition of increasing amounts of Fe³⁺ ion up to 1 equivalent which was clearly noted by the naked eye as well as under a UV lamp (Fig. 12b).

In step 2, we added 1 to 45 equivalents of Fe³⁺ to the *in situ* generated compound 4 in CH₃CN and followed the changes by absorption spectroscopy. Upon the addition of increasing amounts of Fe³⁺ from 1 equivalent to 45 equivalents, the absorption band at 599 nm due to compound 4 was shifted hypsochromically by 62 nm and appeared at 537 nm with a clear isosbestic point at 544 nm (Fig. 13a) supporting the existence of two species. The absorption spectral features of the species formed in the presence of 45 equivalents of Fe³⁺ matched with the absorption features of compound 3 reported earlier.⁵ Furthermore, compound 3 was isolated by column

chromatography and its identity was confirmed by HRMS, ¹H, ¹⁹F and ¹¹B NMR analysis. Under a UV lamp, the isolated compound 3 was highly green fluorescent (Fig. 13b) as reported earlier.⁵ The quantum yield (Φ_f) and singlet state lifetime (τ) of isolated compound 3 were in agreement with the reported data.⁵ We then carried out systematic fluorescence titration studies by adding 1 to 45 equivalents of Fe³⁺ to the *in situ* generated compound 4 in CH₃CN with a time interval of 1 min for each addition. As shown in Fig. 13b, the fluorescence band at 627 nm corresponding to compound 4 experienced a hypsochromic shift by 73 nm and appeared at 554 nm corresponding to compound 3 with a 1000-fold enhancement in the fluorescence intensity, and the intensity enhancement was saturated by the addition of 45 equivalents of Fe³⁺. Although the systematic titration required about 1.5 h for the completion of the reaction, we noted that the conversion of 2a to 3 requires only 5 min upon one time addition of 45 equivalents of Fe³⁺ ion. The sensitivity of Fe³⁺ towards compound 2a was further examined by measuring the lowest concentration of the analyte using the linear dynamic response. The limit of detection (LOD) was found to be 126 nM (Fig. S24†). However, similar titration experiments in phosphate buffer solution (PBS) failed indicating that compound 2a cannot be used for sensing Fe³⁺ ion in water. All these observations suggest that compound 2a exhibits two stages of fluorescence enhancement depending on the amount of Fe³⁺. We also carried out fluorescence titration studies with the addition of Fe²⁺. However, the addition of excess amounts of Fe²⁺ to compound 2a resulted in the formation of only compound 4 but not compound 3 indicating that compound 2a doesn't exhibit a two step fluorescence enhanced chemodosimetric sensing behaviour towards Fe²⁺. The hydrolysis of dinitrophenylhydrazone in

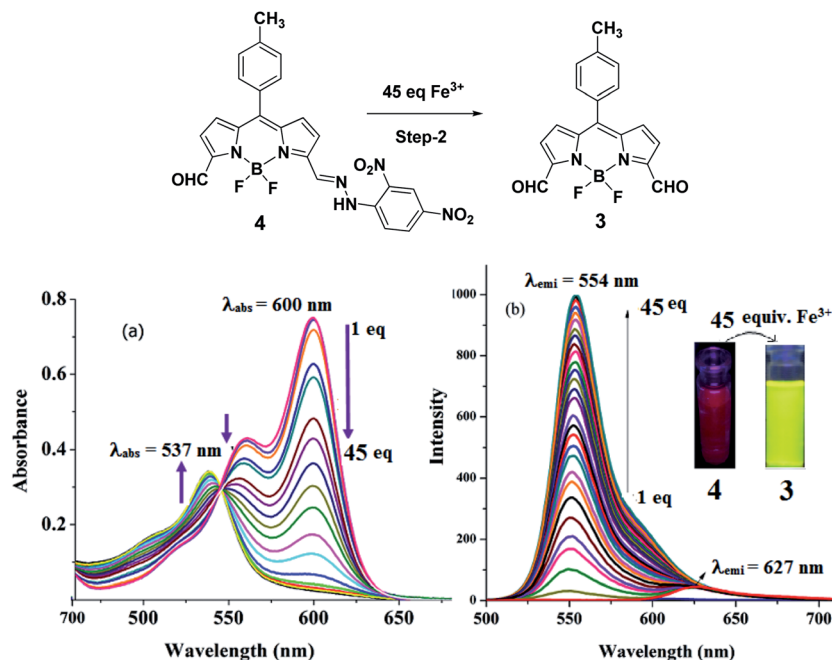


Fig. 13 (a) Absorption and (b) emission spectral changes of BODIPY 2a (10 μ M) upon titration with 1–45 equivalents of Fe³⁺ ($\lambda_{\text{ex}} = 488$ nm) in CH₃CN. (Inset: fluorescence colour change of 2a UV lamp ($\lambda_{\text{ex}} = 365$ nm) upon addition of 45 equivalents of Fe³⁺.)

compound 2a was expected in the presence of Fe³⁺ since it is well established that Fe³⁺ can hydrolyze Schiff bases by metal promoted hydrolysis mechanism.¹³ Thus, we conclude that compound 2a can only be used as a two step fluorescence enhanced chemodosimetric sensor for Fe³⁺. To test the sensitivity of compound 2a, we also carried out systematic absorption studies on compound 2a in an acetate buffer solution over a pH range of 2.2–13 (Fig. S23[†]). The absorption spectra of compound 2a as a function of the pH in an acetate buffer solution exhibited decrease in the intensity of the respective absorption bands with increasing pH without significant changes in the peak maxima. Since the absorption band of compound 2a was already bathochromically shifted and appeared at 613 nm in a highly polar aqueous medium compared to other non-polar solvents like toluene and chloroform, no significant shifts in the absorption peak maxima were expected with a change in pH of the buffer medium. As the pH increased, the changes in the intensity of the absorption bands were minimal. Similarly, the emission studies of compound 2a also showed a significant decrease in the intensity of the fluorescence band with negligible shifts in the peak maxima at different pH.

Conclusions

In summary, we used 3,5-diformyl BODIPY to synthesize symmetrical and unsymmetrical substituted BODIPYs with phenylhydrazone/2,4-dinitrophenylhydrazone and acetal groups at the 3- and 5-positions under simple reaction conditions. The crystal structure of the solved unsymmetrical BODIPY with acetal and 2,4-dinitrophenylhydrazone substituents at the 3- and 5-positions, respectively, revealed that the substituents are in

extended conjugation with the BODIPY unit. Both symmetrical and unsymmetrical BODIPYs absorb and emit at ~ 600 nm with low quantum yields. The absorption properties of BODIPYs in DMSO and DMF solvents were distinctly different from those in other solvents. The unsymmetrical BODIPY was shown to act as a sensor for F⁻, CH₃COO⁻ and H₂PO₄⁻ by means of a deprotonation mechanism. Because of the two different substituents, the unsymmetrical BODIPY dye was shown to have the unique ability of acting as a two step fluorescence enhanced chemodosimetric sensor for Fe³⁺ unlike other reported⁹ Fe³⁺ chemodosimetric sensors. This feature enables the unsymmetrical BODIPY dye 2a to be used for the detection of different amounts of Fe³⁺ in solution.

Experimental section

General

Chemicals. All general chemicals and solvents were procured from S.D. Fine Chemicals, India. Column chromatography was performed using silica gel obtained from Sisco Research Laboratories, India. All the solvents used were of analytical grade and were purified and dried by routine procedures immediately before use.

Instrumentation. All the NMR spectra (δ values, ppm) were recorded with a 400 MHz spectrometer. Tetramethylsilane (TMS) was used as an external reference for recording ¹H (of residual proton; $\delta = 7.26$ ppm) and ¹³C ($\delta = 77.2$ ppm) spectra in CDCl₃. Chemical shift multiplicities are reported as s = singlet, d = doublet, t = triplet, q = quartet and m = multiplet. ¹¹B and ¹⁹F NMR spectra were recorded on Bruker spectrometer operated at 128.3 and 376.4 MHz. All the NMR measurements were

carried out at room temperature in deuteriochloroform (CDCl_3). The HRMS spectra were recorded with a Bruker maxis impact 282 001.00081 and Q-ToF micro mass spectrometer using the electron spray ionization method, TOF analyser. Absorption and steady state fluorescence spectra were recorded with Varian Cary-Eclipse instruments. For UV-vis and fluorescence titrations, a stock solution of BODIPY 2 (5×10^{-6} M, 1×10^{-5} M) was prepared by using HPLC grade acetonitrile (CH_3CN). The quantum yields (Φ_f) were calculated using sulforhodamine reference ($\Phi = 0.69$ in ethanol, $\lambda_{\text{exc}} = 530$ nm)¹⁴ for compound 1 and 3 in CH_3CN . All Φ_f are corrected for changes in refractive index. All the anions were used as tetrabutylammonium salts and cations were used as perchlorate salts. The tetrabutylammonium fluoride (TBAF), tetrabutylammonium acetate, sodium dihydrogen phosphate (NaH_2PO_4) and iron perchlorate ($\text{Fe}(\text{ClO}_4)_3 \cdot x\text{H}_2\text{O}$) solutions were prepared (1×10^{-2} M) in CH_3CN . The association constant of the anionic complex formed in solution was estimated using the standard Benesi-Hildebrand equation. The limit of detection (LOD) for the Fe^{3+} ions was calculated to be three times the standard deviation for the average measurements of ten blank samples by the slope ($\text{LOD} = 3\sigma/K$).¹⁵ The solution containing BODIPY 1 ($10 \mu\text{M}$) was placed in a quartz cell (1 cm width), and anion, Fe^{3+} solutions were added in an incremental fashion. Their corresponding UV-vis and fluorescence spectra were recorded at 298 K. For ^1H NMR titration, the spectra were measured using the 400 MHz NMR spectrometer. A solution of 2a in CD_3CN was prepared (2×10^{-2} M), and a 0.4 ml portion of this solution was transferred into a 5 mm NMR tube. A small aliquot of TBAF in CD_3CN was added in an incremental fashion, and their corresponding spectra were recorded.

X-ray diffraction studies

A single crystal X-ray structural study was performed using a CCD Oxford Diffraction XCALIBUR-S diffractometer equipped with an Oxford Instrument with a low-temperature attachment. Data were collected at 150(2) K using graphite-monochromated Mo- K_α radiation ($\lambda_x = 0.71073$ Å). The strategy for the data collection was evaluated by using the CrysAlisPro CCD software. The data were collected by standard 'phi-omega scan' techniques and were scaled and reduced using CrysAlisPro RED software. Structure solutions for compound 1 was obtained using direct methods (SHELXS-97)¹⁶ and refined using full-matrix least-squares methods on F^2 using SHELXL-97.¹⁷ The positions of all the atoms were obtained by direct methods. All non-hydrogen atoms were refined anisotropically. The hydrogen atoms were placed in geometrically constrained positions and refined with isotropic temperature factors, generally 1.2 Ueq. of their parent atoms.†

Synthesis of compounds

Method 1. A solution of compound 3 (0.04 mmol) in ethanol (10 ml) was added dropwise to a solution of phenylhydrazine/2,4-nitrophenylhydrazine (0.08 mmol) in ethanol (20 ml) with stirring at reflux. After stirring for 6 h, the solvent was removed by evaporation and the resultant crude compound was purified

by alumina column chromatography using petroleum ether-ethylacetate (94 : 6) to afford the pure compound as a blue solid.

Method 2. A solution of compound 3 (0.04 mmol) in ethanol (10 ml) was added dropwise to a solution of 2,4-nitrophenylhydrazine (0.08 mmol) in ethanol (20 ml) with stirring overnight at room temperature. The solvent was removed by evaporation and the resultant crude compound was purified by alumina column chromatography using petroleum ether-ethylacetate (94 : 6) to afford the pure compound as a blue solid.

Compound 1. Yield 62%. ^1H NMR (400 MHz, CDCl_3 , δ in ppm) 2.47 (s, 3H, CH_3), 6.81 (d, $J = 4.40$ Hz, 2H, py), 6.92 (t, $J = 7.34$ Hz, 2H, ph), 7.09–7.15 (m, 6H, ph + py), 7.24–7.33 (m, 6H, ph), 7.41 (d, $J = 8.07$ Hz, 2H, Ar), 8.20 (s, 2H, aldehyde-CH), 8.49 (s, 2H, NH); ^{13}C NMR (100 MHz, CDCl_3 , δ in ppm) 21.60, 113.56, 117.24, 121.64, 129.21, 129.37, 129.50, 130.65, 131.69, 140.29, 143.38, 151.62. ^{19}F NMR (376.49 MHz, CDCl_3 , δ in ppm) –138.03 (q, $J(\text{F}, \text{B}) = 64.0$ Hz); ^{11}B NMR (128.38 MHz, CDCl_3 , δ in ppm) 1.13 (t, $J(\text{B}, \text{F}) = 30.8$ Hz); HRMS calcd for ($\text{C}_{30}\text{H}_{25}\text{BF}_2\text{N}_6\text{Na}$) 519.2280 ($\text{M} + \text{H}$)⁺, found 519.2290 ($\text{M} + \text{H}$)⁺.

Compound 2a. Yield: 17%. ^1H NMR (400 MHz, CDCl_3 , δ in ppm) 1.26 (t, 6H, CH_3), 2.49 (s, 3H, tol- CH_3), 3.68–3.77 (m, 2H, CH_2), 3.78–3.87 (m, 2H, CH_2), 5.99 (s, 1H, CH), 6.80 (d, $J = 4.40$ Hz, 1H), 6.93 (d, $J = 4.40$ Hz, 1H, py), 6.97 (d, $J = 4.40$ Hz, 1H, py), 7.18 (d, $J = 4.03$ Hz, 1H, py), 7.35 (d, $J = 8.07$ Hz, 2H, Ar), 7.45 (d, $J = 8.07$ Hz, 2H, Ar), 8.09 (d, $J = 9.54$ Hz, 1H, ph), 8.38 (dd, $J = 9.54, 2.20$ Hz, 1H, ph), 8.61 (s, 1H, aldehyde-CH), 9.17 (d, $J = 2.57$ Hz, 1H, ph), 11.55 (s, 1H, NH); ^{13}C NMR (100 MHz, CDCl_3 , δ in ppm) 15.38, 21.66, 63.36, 99.64, 117.20, 117.89, 118.63, 123.51, 129.46, 130.15, 130.44, 130.75, 130.94, 132.31, 135.80, 136.78, 139.45, 141.63, 144.07, 146.03, 148.96, 159.35; ^{19}F NMR (376.49 MHz, CDCl_3 , δ in ppm) –137.96 (q, $J(\text{F}, \text{B}) = 64.0$ Hz); ^{11}B NMR (128.38 MHz, CDCl_3 , δ in ppm) 0.93 (t, $J(\text{B}, \text{F}) = 30.8$ Hz); HRMS calcd for ($\text{C}_{28}\text{H}_{27}\text{BF}_2\text{N}_6\text{O}_6\text{Na}$): 615.1951 ($\text{M} + \text{Na}$)⁺, found 615.1961 ($\text{M} + \text{Na}$)⁺.

Compound 2b. Yield 26%. ^1H NMR (400 MHz, CDCl_3 , δ in ppm) 2.49 (s, 3H, CH_3), 3.52 (s, 6H, CH_3), 5.87 (s, 1H, CH), 6.76 (d, $J = 4.27$ Hz, 1H, py), 6.96 (t, $J = 4.58$ Hz, 1H, py), 7.20 (d, $J = 4.58$ Hz, 1H, py), 7.36 (d, $J = 7.63$ Hz, 1H, Ar), 7.46 (d, $J = 7.93$ Hz, 1H, Ar), 8.10 (d, $J = 9.77$ Hz, 1H, ph), 8.39 (dd, $J = 9.46, 2.44$ Hz, 1H, ph), 8.63 (s, 1H, CH), 9.17 (d, $J = 2.44$ Hz, 1H, ph), 11.57 (s, 1H, NH); ^{13}C NMR (100 MHz, CDCl_3 , δ in ppm) 21.68, 54.64, 98.49, 117.20, 1128.14, 118.55, 123.51, 129.48, 130.15, 130.44, 130.79, 130.91, 132.01, 135.87, 139.32, 141.73, 144.03, 146.21, 149.26, 157.72; ^{19}F NMR (376.49 MHz, CDCl_3 , δ in ppm) –138.44 (q, $J(\text{F}, \text{B}) = 64.0$ Hz); ^{11}B NMR (128.38 MHz, CDCl_3 , δ in ppm) 0.92 (t, $J(\text{B}, \text{F}) = 30.8$ Hz); HRMS calcd for ($\text{C}_{26}\text{H}_{23}\text{BF}_2\text{N}_6\text{O}_6\text{Na}$): 587.1638 ($\text{M} + \text{Na}$)⁺, found 587.1636 ($\text{M} + \text{Na}$)⁺.

Acknowledgements

MR and VL acknowledge the financial support from the Council of Scientific and Industrial Research, Govt. of India.

References

- (a) G. Ulrich, R. Ziessel and A. Harriman, *Angew. Chem., Int. Ed.*, 2008, 47, 1184–1201; (b) A. Loudet and K. Burgess, *Chem.*

- Rev.*, 2007, **107**, 4891–4932; (c) R. Ziessel, G. Ulrich and A. Harriman, *New J. Chem.*, 2007, **31**, 496–501.
- 2 (a) A. Kamkaew, S. H. Lim, H. B. Lee, L. V. Kiew, L. Y. Chung and K. Burgess, *Chem. Soc. Rev.*, 2013, **42**, 77–88; (b) N. Boens, V. Leen and W. Dehaen, *Chem. Soc. Rev.*, 2012, **41**, 1130–1172; (c) G. Duran-Sampedro, A. R. Agarrabeitia, I. Garcia-Moreno, A. Costela, J. Bañuelos, T. Arbeloa, I. López Arbeloa, J. L. Chiara and M. J. Ortiz, *Eur. J. Org. Chem.*, 2012, 6335–6350; (d) V. Leen, D. Miscoria, S. Yin, A. Filarowski, J. Molisho Ngongo, M. Van der Auweraer, N. Boens and W. Dehaen, *J. Org. Chem.*, 2011, **76**, 8168–8176; (e) V. Leen, T. Leemans, N. Boens and W. Dehaen, *Eur. J. Org. Chem.*, 2011, **2011**, 4386–4396.
- 3 (a) V. Lakshmi and M. Ravikanth, *Chem. Phys. Lett.*, 2013, **564**, 93–97; (b) V. Lakshmi and M. Ravikanth, *J. Org. Chem.*, 2011, **76**, 8466–8471; (c) L. Jiao, W. Pang, J. Zhou, Y. Wei, X. Mu, G. Bai and E. Hao, *J. Org. Chem.*, 2011, **76**, 9988–9996; (d) A. Harriman, M. A. H. Alamiry, J. P. Hagon, D. Hablot and R. Ziessel, *Angew. Chem., Int. Ed.*, 2013, **5**, 6611–6615; (e) T. Bura, P. Retailleau and R. Ziessel, *Angew. Chem., Int. Ed.*, 2010, **49**, 6659–6663.
- 4 (a) E. Heyer and R. Ziessel, *Tetrahedron Lett.*, 2013, **54**, 3388–3393; (b) R. Ziessel, G. Ulrich, A. Haefele and A. Harriman, *J. Am. Chem. Soc.*, 2013, **135**, 11330–11344; (c) A. Mirloup, P. Retailleau and R. Ziessel, *Tetrahedron Lett.*, 2013, **54**, 4456–4462; (d) S.-L. Niu, C. Massif, G. Ulrich, P.-Y. Renard, A. Romieu and R. Ziessel, *Chem. – Eur. J.*, 2012, **18**, 7229–7242; (e) J. Suk, K. M. Omer, T. Bura, R. Ziessel and A. J. Bard, *J. Phys. Chem. C*, 2011, **115**, 15361–15368; (f) G. Ulrich, S. B. Goeb, A. De Nicola, P. Retailleau and R. Ziessel, *J. Org. Chem.*, 2011, **76**, 4489–4505.
- 5 S. Madhu, M. R. Rao, M. S. Shaikh and M. Ravikanth, *Inorg. Chem.*, 2011, **50**, 4392–4400.
- 6 S. Madhu, S. K. Basu, S. Jadhav and M. Ravikanth, *Analyst*, 2013, **138**, 299–306.
- 7 S. Madhu and M. Ravikanth, *Inorg. Chem.*, 2012, **51**, 4285–4292.
- 8 (a) V. Lakshmi and M. Ravikanth, *J. Org. Chem.*, 2013, **78**, 4993–5000; (b) S. Zhu, J. Bi, G. Vegesna, J. Zhang, F.-T. Luo, L. Valenzano and H. Liu, *RSC Adv.*, 2013, **3**, 4793–4800; (c) S. Zhu, J. Zhang, J. Janjanam, G. Vegesna, F.-T. Luo, A. Tiwari and H. Liu, *J. Mater. Chem. B*, 2013, **1**, 1722–1728; (d) J. Zhang, S. Zhu, L. Valenzano, F.-T. Luo and H. Liu, *RSC Adv.*, 2013, **3**, 68–72; (e) S. Zhu, J. Zhang, G. Vegesna, A. Tiwari, F.-T. Luo, M. Zeller, R. Luck, H. Li, S. Green and H. Liu, *RSC Adv.*, 2012, **2**, 404–407; (f) S. Zhu, J. Zhang, G. K. Vegesna, R. Pandey, F.-T. Luo, S. A. Green and H. Liu, *Chem. Commun.*, 2011, **47**, 3508–3510.
- 9 (a) M. Shellaiah, Y.-H. Wu, A. Singh, M. V. Ramakrishnam Raju and H.-C. Lin, *J. Mater. Chem. A*, 2013, **1**, 1310–1318; (b) R. K. Pathak, J. Dessingou, V. K. Hinge, A. G. Thawari, S. K. Basu and C. P. Rao, *Anal. Chem.*, 2013, **85**, 3707–3714; (c) R.-L. Liu, H.-Y. Lu, M. Li, S.-Z. Hu and C.-F. Chen, *RSC Adv.*, 2012, **2**, 4415–4420; (d) L. Huang, F. Hou, J. Cheng, P. Xi, F. Chen, D. Bai and Z. Zeng, *Org. Biomol. Chem.*, 2012, **10**, 9634–9638; (e) Z. Aydin, Y. Wei and M. Guo, *Inorg. Chem. Commun.*, 2012, **20**, 93–96; (f) L. Zhang, J. Wang, J. Fan, K. Guo and X. Peng, *Bioorg. Med. Chem. Lett.*, 2011, **21**, 5413–5416.
- 10 H. L. Kee, C. Kirmaier, L. Yu, P. Thamyongkit, W. J. Youngblood, M. E. Calder, L. Ramos, B. C. Noll, D. F. Bocian, W. R. Scheidt, R. R. Birge, J. S. Lindsey and D. Holten, *J. Phys. Chem. B*, 2005, **109**, 20433–20443.
- 11 (a) P. Bose, B. N. Ahamed and P. Ghosh, *Org. Biomol. Chem.*, 2011, **9**, 1972–1979; (b) B. Zhang, Y. Li and W. Sun, *Eur. J. Inorg. Chem.*, 2011, 4964–4969; (c) J. Shao, X. Xudong Yu, X. Xu, H. Lin, Z. Zunsheng Cai and H. Lin, *Talanta*, 2009, **79**, 547–551; (d) S. Hu, Y. Guo, J. Xu and S. Shao, *Org. Biomol. Chem.*, 2008, **6**, 2071–2075.
- 12 J. A. Dean, *Lange's Handbook of Chemistry*, McGraw-Hill, New York, 13th edn, 1987, p. 15 (section 5).
- 13 (a) A. K. Singh and N. J. Majumdar, *J. Photochem. Photobiol., B*, 1997, **39**, 140–145; (b) R. Alarcon, M. Silva and M. Valcareal, *Anal. Lett.*, 1982, **15**, 891–907.
- 14 P. C. Beaumont, D. G. Johnson and B. J. J. Parsons, *J. Chem. Soc., Faraday Trans.*, 1998, **94**, 195–199.
- 15 (a) L. G. Hepler and G. Olofsson, *Chem. Rev.*, 1975, **75**, 585–602; (b) J.-L. Burgot, *Ionic Equilibria in Analytical Chemistry*, Springer, New York, USA, 2012.
- 16 G. M. Sheldrick, *SHELXS-97, Program for crystal structure solution*, University of Göttingen: Göttingen, Germany, 1997.
- 17 G. M. Sheldrick, *SHELXL-97, Program for crystal structure refinement*, University of Göttingen, Göttingen, Germany 1997.